Supporting Information for
Ferromagnetic MnSn monolayer epitaxially grown on silicon substrate

Qian-Qian Yuan(袁茜茜)[1], Zhaopeng Guo(郭照芃)[1], Zhi-Qiang Shi(石志强)[1], Hui Zhao(赵辉)[1], Zhen-Yu Jia(贾振宇)[1], Qianjin Wang(王前进)[1], Jian Sun(孙建)[1,2], Di Wu(吴镝)[1,2], Shao-Chun Li(李绍春)[1, 2,3]**

[1] *National Laboratory of Solid State Microstructures, School of Physics, Nanjing University, Nanjing 210093, China*

[2] *Collaborative Innovation Center of Advanced Microstructures, Nanjing University, Nanjing 210093, China*

[3] *Jiangsu Provincial Key Laboratory for Nanotechnology, Nanjing University, Nanjing 210093, China*

** Corresponding authors: scli@nju.edu.cn (S.-C. Li)

Methods

Molecular beam epitaxy growth. Monolayer and few-layered MnSn films were grown on the Si(111) substrate. The Si(111) single crystal was loaded into ultrahigh vacuum and then outgassed at ~600 °C overnight. The Si(111)-7×7 surface was obtained through cycles of flash annealing up to ~1200 °C. The Sn/Si(111)-$2\sqrt{3} \times 2\sqrt{3}$ buffer layer was firstly prepared on the Si(111)-7×7 surface by depositing ~1 ML (1 ML equals to 7.8×10^{14} atoms / cm^2) Sn followed by annealing to ~600 °C. The quality of the Sn/Si(111)-$2\sqrt{3} \times 2\sqrt{3}$ buffer layer was checked by STM prior to MnSn growth. The Mn and Sn with a flux ratio of ~1:1 were then deposited onto the Sn/Si(111)-$2\sqrt{3} \times 2\sqrt{3}$ surface with the substrate kept at RT. Uniform and high quality MnSn monolayers were obtained after annealing up to ~300 °C.

Scanning tunneling microscopy/spectroscopy characterization. STM/STS measurements were *in situ* carried out with a commercial STM system (USM1500, UNISOKU) at both ~4.2 K and ~78 K. The base pressure is 1×10^{-10} mbar. A mechanically cut Pt-Ir tip was adopted for scan. The STM images were collected under the constant current mode. The dI/dV data were taken via a lock-in amplifier with the ac modulation of 6 mV and 879 Hz.

XPS characterization. XPS measurements were perforemed with a commercial XPS system (PHI 5000 Versa Probe, UlVAC-PHI). The base pressure is less than 6×10^{-10} mbar. The Al Kα x-ray was used as the excitation source. The photon energies were calibrated via the bind energy of C 1s. The MnSn film of ~5 nm thick was used for the XPS measurement. Ag capping layer of ~4 nm was grown on MnSn film to protect the sample from exposure

to air.

Magnetic properties measurements. The magnetic properties were measured with a SQUID magnetometer (Quantum Design) configured with a longitudinal pick-up coil. The applied magnetic fields were in-plane oriented. Before exposed in air, the MnSn film was covered by Sn capping layers of ~20 nm thick to prevent from oxidation.

DFT calculations. Crystal structure is predicted using a machine learning accelerated crystal structure searching program [1,2]. Thousands of crystal structure of MnSn are generated using the crystal structure searching program with some constrains based on some information from the experimetntal side to accelerate the searching process. All the crystal structures are optimized in ferromagnetic state considering the ferromagnetic signal in experiments. We optimized the lattice constants and atom positions using the Vienna ab-initio simulation package (VASP) [3]. The Perdew-Burke-Ernzerhof (PBE) [4] generalized gradient approximation (GGA) exchange-correlation functional are performed in project augmented wave (PAW) method [5]. We applied a kinetic energy cutoff of 370 eV for plane wave basis. And k-point meshes of 6 × 6 × 12 and 6 × 6 × 1 Monkhorst-Pack grid [6] were set for bulk and monolayer calculations, respectively. In the electronic structure calculations, the DFT+U method in Dudarev's approach [7] is employed. An effective Hubbard U_{eff}(U-J) parameter of 2.0 eV is applied for Mn atoms. A vaccum space of 20 Å in c direction is implemented to model the monolayer sturcture. A supercell of 2 × 2 × 2 is constructed to calculate phonon spectra using PHONOPY package [8].

References：

[1] Xia K, Gao H, Liu C, Liu J, Yuan J, Sun J, Wang H-T and Xing D 2018 Sci. Bull. **63** 817-824
[2] Wang X, Wu J, Wang J, Chen T, Gao H, Chen Q, Ding C, Wen J, Sun J 2018 Phys. Rev. B **98** 174112
[3] Kresse G and Furthmüller J 1996 Phys. Rev. B **54** 11169
[4] Perdew J P, Burke K and Ernzerhof M1996 Phys. Rev. Lett. **77** 3865
[5] Kresse G and Joubert D 1999 Phys. Rev. B **59** 1758
[6] Chadi D J, 1997 Phys. Rev. B **16** 1746
[7] Dudarev S L, Botton G A, Savrasov S Y, Humphreys C J and Sutton A P, 1998 Phys. Rev. B **57** 1505
[8] Togo A, and Tanaka I 2015 Scripta Mater. **108** 1

The lattice compatibility between MnSn and Si substrate.

The atomic resolution images of the MnSn islands and the exposed Sn buffer layer as displayed in Fig. S1 indicate that the lattices of them are compatible. The relative lattice orientation of MnSn, Sn/Si(111)-$2\sqrt{3} \times 2\sqrt{3}$ buffer layer and Si substrate is sketched in Fig. S1(d). After optimizing growth temperature, MnSn films grown in layer-by-layer style can be obtained, as shown in Fig. S2. The relative coverages of each layer on the samples with nominal thickness of 1L, 2L, 3L and 4L are established and consequently the real coverages of them are accurately determined to be 1.1 ML, 1.9 ML, 2.9 ML and 3.8 ML respectively.

Electronic properties of MnSn films.

When temperature is reduced from ~78 K to ~4.2 K, a tiny dip is observed near the Fermi energy in the dI/dV spectra, as presented in Fig. S3 and Fig. 1(h) in the main text. The dip may be originated from the electron-electron correlation effect. However, the according STM images taken at 4.2 K and 78 K are the same (Fig. S4). This evidences that there is no phase transition happened.

Origin of the main defects observed in MnSn monolayer.

Figures S5(a) and 5(b) show the zoom-in images of two kinds of defects, A and B as assigned in the main text. Figures S5(c)-5(d) show the atomic structures of the adsorbed Sn atom and Mn interstitial atom, and Figs. S5(e)-5(f) the simulated STM topographic images based on structure of Figs. S5(c)-5(d) respectively. The simulations are consistent with the experimental STM results. This agreement further verifies the validity of the DFT optimized structure of MnSn monolayer.

SQUID magnetization measurements background subtraction.

The raw data of magnetization curves and magnetic hysteresis loops (Fig. S6) show obvious diamagnetic background contributions, which come from the diamagnetic Si substrate and the Sn capping layer. The n-type Si substrate directly covered by ~20-nm-thick Sn capping layer without the MnSn film was also measured to obtain the total diamagnetic background signals. Additionally, the paramagnetic signals from the magnetic Mn defects should also be ruled out. We adopted the same method mentioned in the reference (Dante Jamal O'Hara, et al., *IEEE Magnetics Letters* **2018**, *9*, 1405805) for the background subtraction. As an example, the procedure of background subtraction for the 4-layer-thick MnSn is illustrated in Fig. S7. The measured background data was used to be subtracted from the raw data for the MnSn film (Fig. S7(b)). Figure S7(c) shows the result after the background is subtracted. Similarly, for magnetic hysteresis loops, the linear parts

besides the ferromagnetic loop also reveal the diamagnetic response. The diamagnetic, paramagnetic components and result of subtraction are displayed in Figure S7(e)-7(f).

Details of the DFT optimized MnSn structure.

All the details about the atom coordinates are illustrated in Table S1. The space group of bulk MnSn crystal is *P-62m* (No. 189). The calculated lattice constants are a = b = 6.5764 Å and c = 2.9097 Å. The nearest neighbor Mn-Mn atoms are located in the same layer. The nearest neighbor Sn-Sn atoms are located in different layers, and the distance of nearest neighbor Sn-Sn atoms is 2.910 Å, same to the length of c axis. The distance of nearest neighbor Mn-Sn atoms is 2.771 Å.

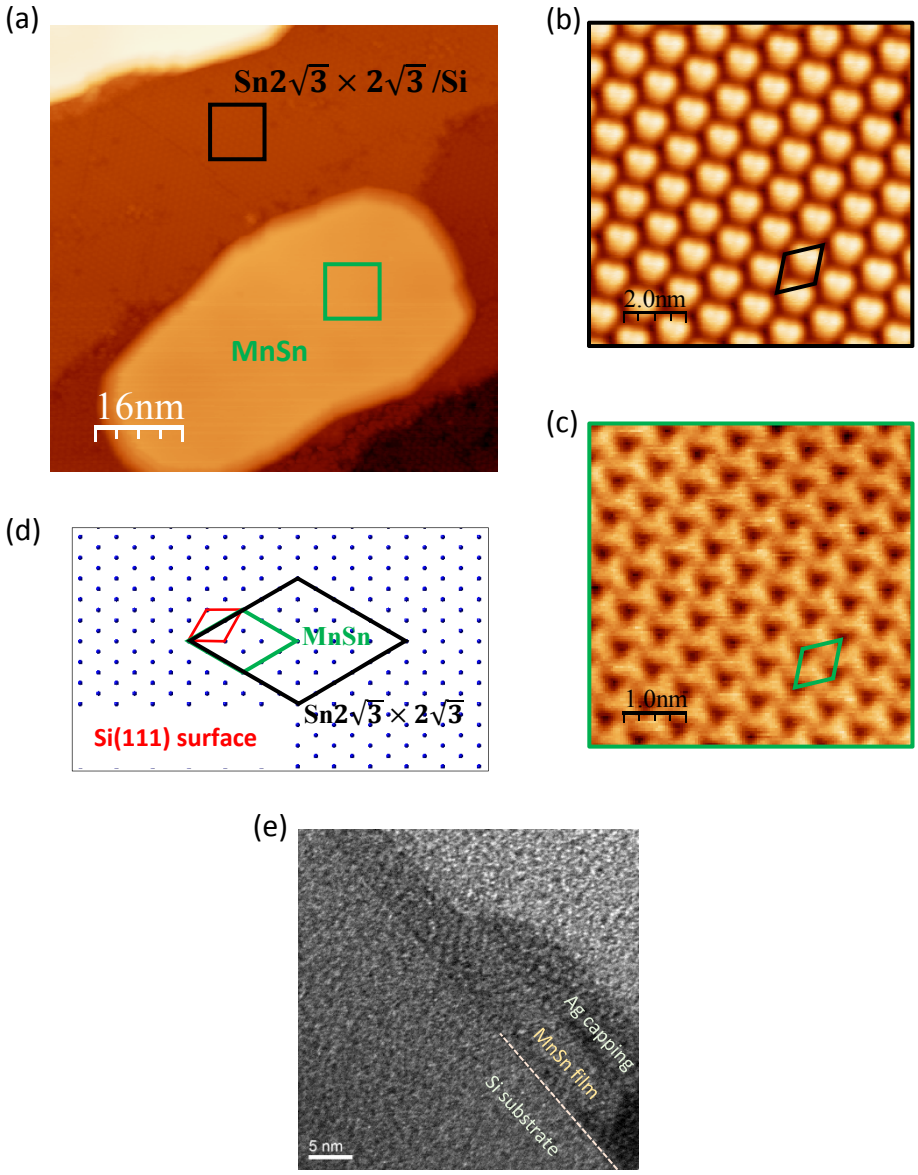

Figure S1. The compatible lattices of MnSn islands and Sn buffer layer. (a) A large scale STM image (80 × 80 nm^2, U = +2.0 V, I_t = 50 pA) of MnSn islands with the Sn/Si(111)-$2\sqrt{3} \times 2\sqrt{3}$ buffer layer exposed. This island's height is about 1.68 nm. (b, c) Atomic resolutions of Sn/Si(111)$2\sqrt{3} \times 2\sqrt{3}$ buffer layer and MnSn islands. The rhombuses mark the unit cells. The scale bar of image in (c) is half of image in (b). (d) The relative lattice arrangement of MnSn, Sn buffer layer and Si substrate. The red, black and green colored rhombuses represent surface unit cells of Si(111)-(1 × 1), Sn/Si(111)$2\sqrt{3} \times 2\sqrt{3}$ and MnSn. (e) Cross-sectional TEM image of ~6-nm-thick MnSn layer on Si. The Ag capping layer of ~30 nm was grown to protect sample from air. The yellow dashed line indicates the sharp interface.

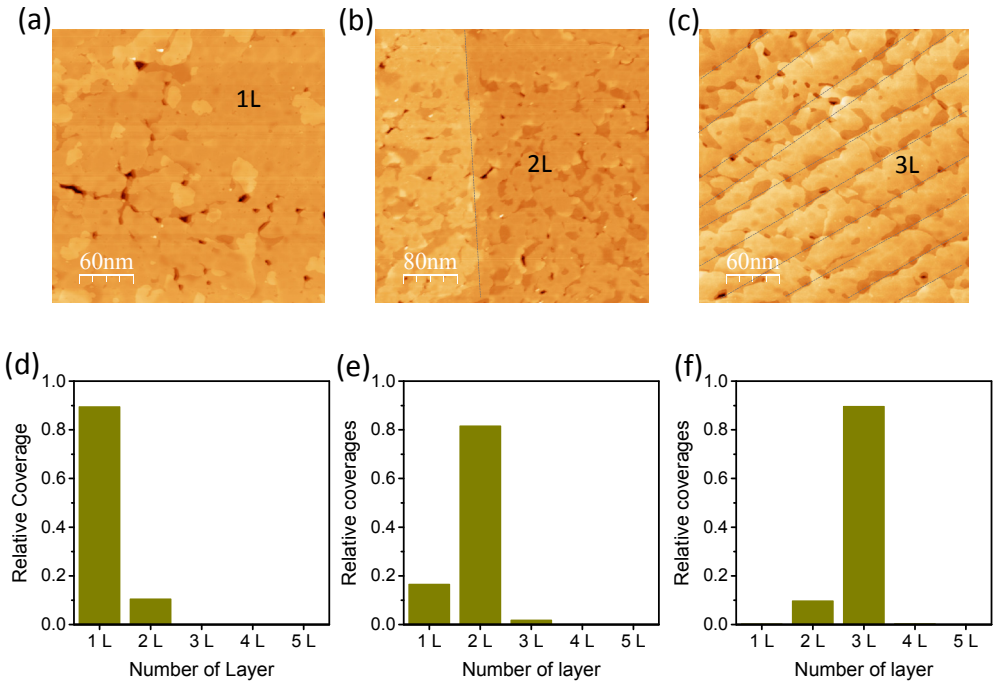

Figure S2. Layer-by-layer growth mode of MnSn and the establishment of layer thicknesses. (a-c) Large-scale STM images of nominal 1L, 2L and 3L MnSn films. All the images were taken at U = +2.0 V and I_t = 100 pA. The dashed lines mark the steps of underlying Si substrates. (d-f) The corresponding statistic results of the relative coverages of 1, 2 and 3-layer regions over the measured areas.

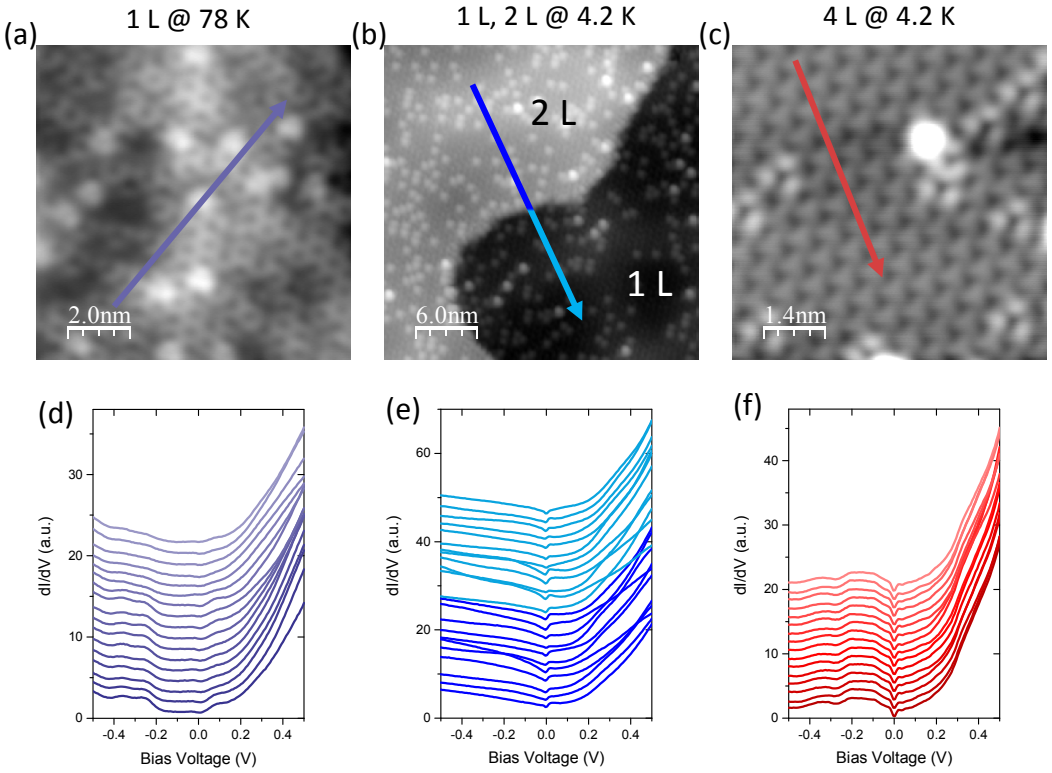

Figure S3. Spatially resolved dI/dV spectra taken on the MnSn films with different thickness at different temperatures. (a) High-resolution STM images of the MnSn monolayer taken at 78 K. (b) STM image taken in the region of the step between 1 L and 2 L at 4.2 K. (c) High-resolution STM image taken on the 4 layered MnSn at 4.2 K. The purple, blue and red arrowed lines indicate the positions where dI/dV spectra were taken. (d-f) The corresponding dI/dV spectra along the arrowed lines marked in (a-c).

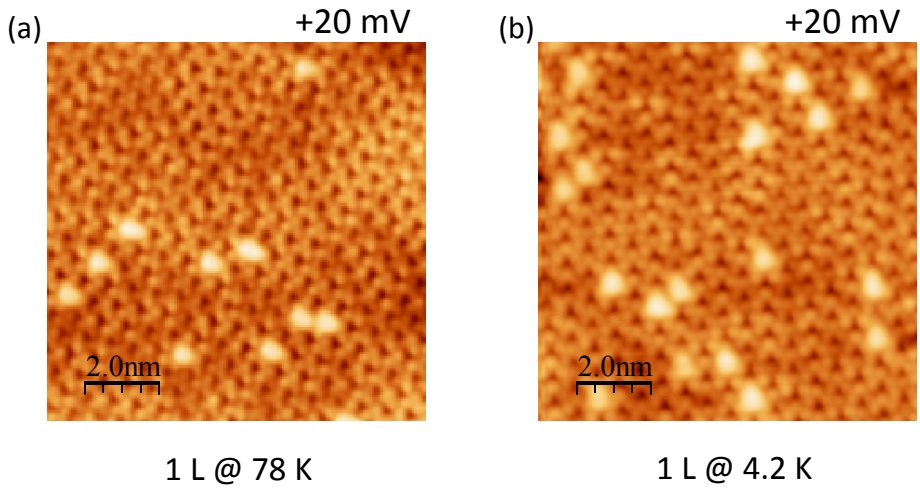

Figure S4. Surface topography of the monolayer MnSn at different temperatures.
(a, b) Topographic images of (10 nm × 10 nm) the monolayer MnSn taken at U = +20 mV at 78 K and 4.2 K respectively. The scale bar is 2 nm.

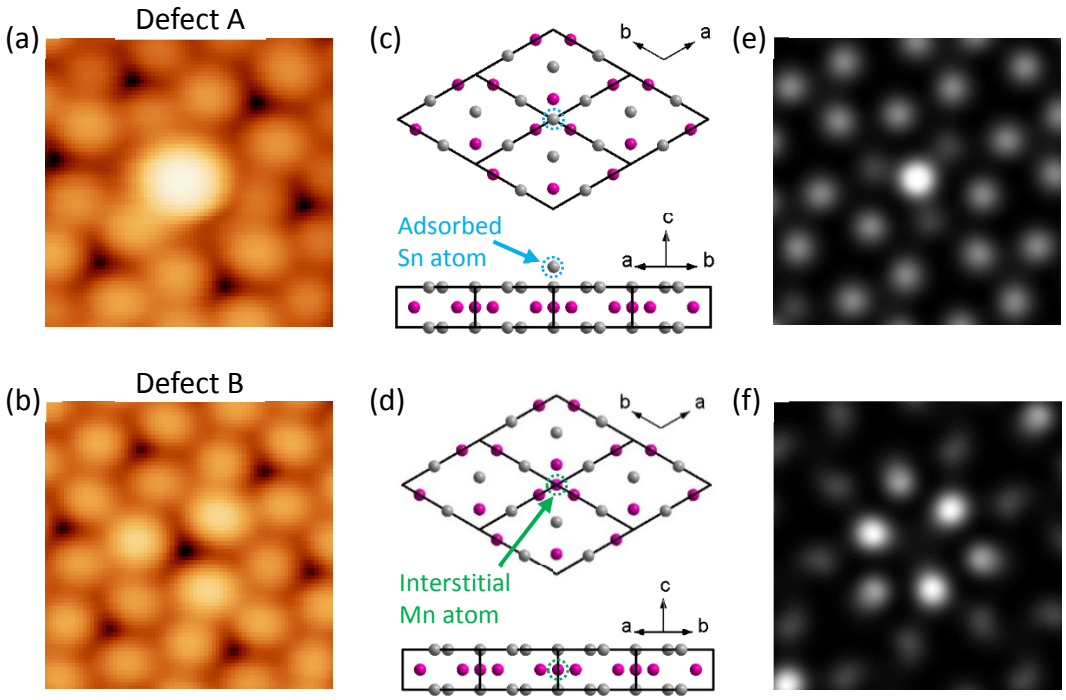

Figure S5. Characterization of the main defects in MnSn monolayer. (a, b) Atomically resolved topographic images of two kinds of defects (size: 1.5×1.5 nm^2). (c, d) Top view and side view of the atomic structures of 2×2×1 supercells with the two corresponding defects. The adsorbed Sn atom and interstitial Mn atom are marked by blue and green dashed circles respectively. (e, f) Simulated STM images of adsorbed Sn atom and Mn interstitial defect based on DFT calculation respectively.

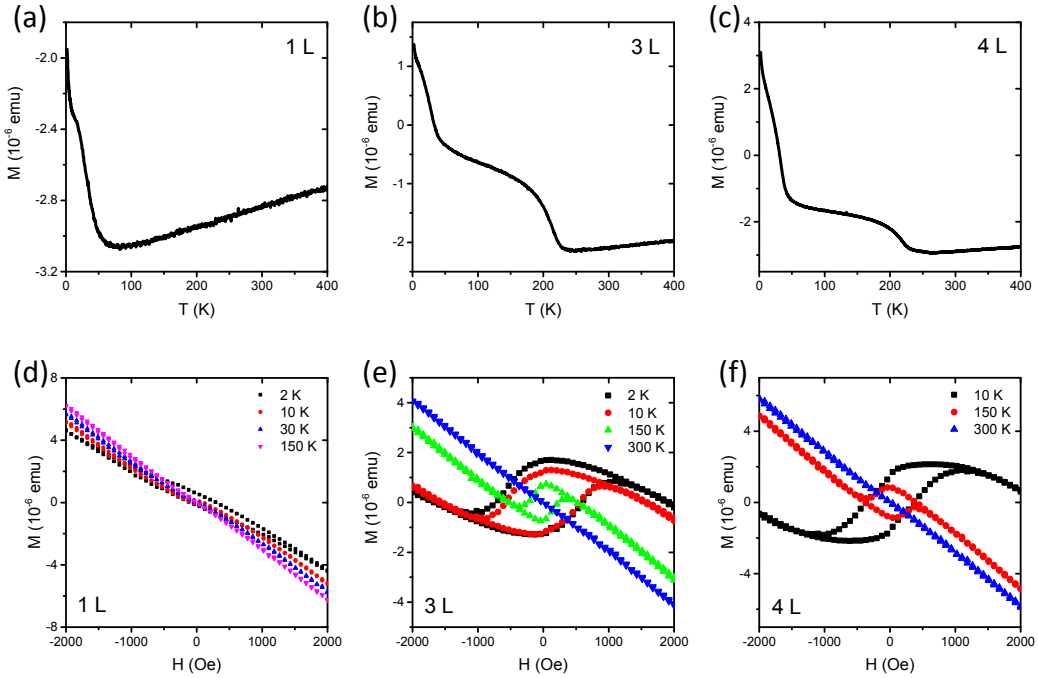

Figure S6. Raw data of the magnetic measurements. (a-c) The magnetization curves as a function of temperature of three samples with thickness of 1L, 3L and 4L MnSn on Si respectively. (d-f) the corresponding magnetic hysteresis loops at various temperatures.

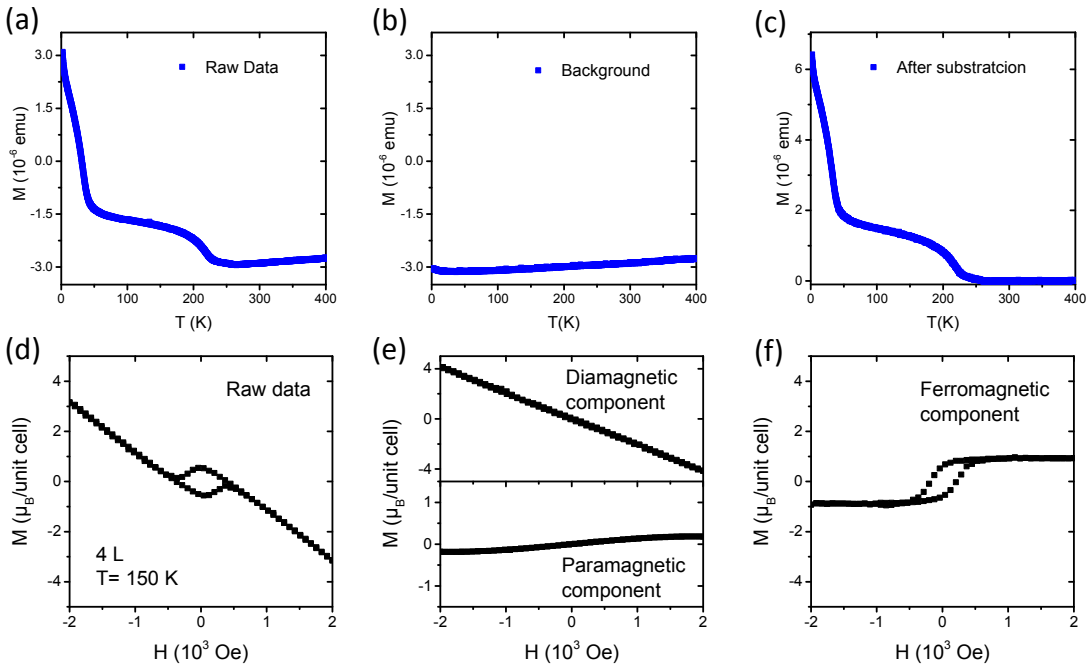

Figure S7. Subtraction of the background from the M~T and M-H data. (a, d) The raw data of magnetization curve and magnetic hysteresis loop taken at 150 K of 4-layer-thick MnSn on Si substrate with ~20-nm-thick Sn capping layer. (b) The measured magnetization curve taken on the bare Si substrate with Sn capping layer. (e) Upper: magnetic hysteresis loop taken at 150 K on the bare Si substrate with Sn capping layer but without MnSn film, which shows diamagnetic background signal. Lower: the extracted paramagnetic component from the raw data. (c, f) Result after subtracting of data in (a, d) by that in (b ,e) respectively.

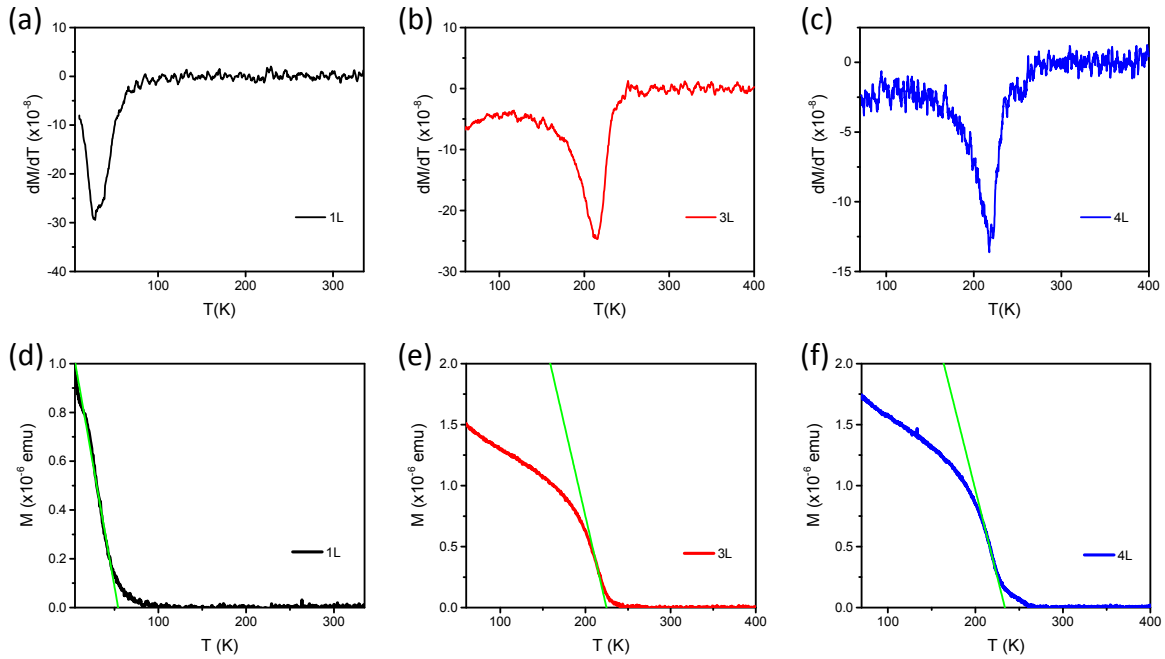

Figure S8. The determination of Curie temperature. (a-c) The derivative curves of magnetizations (dM/dT) for 1L, 3L and 4L respectively. The sharp negative peaks are identified at 31 K, 213.5 K and 218.3 K. (d-f) The magnetization curves with tangents (in green) taken at the points where the dM/dT negative peaks located. The extrapolation of tangents to zero determine Tc to be 54 K, 225 K and 235 K for 1L, 3L and 4L respectively.

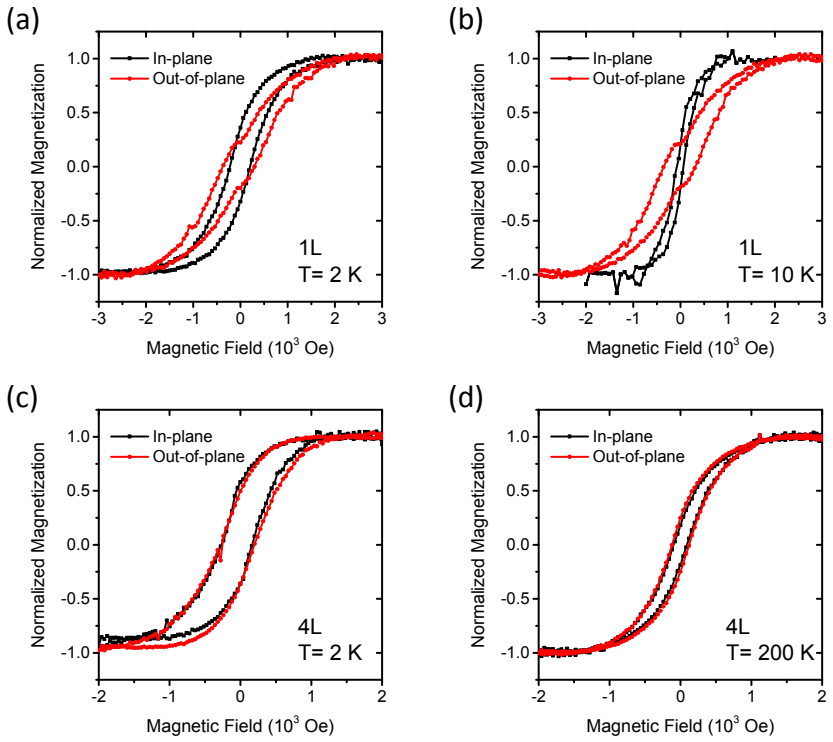

Figure S9. Magnetic anisotropy characterization of MnSn films with different thickness. (a, b) The normalized in-plane and out-of-plane magnetic hysteresis loops of 1L measured at 2 K and 10 K respectively. (c, d) The normalized in-plane and out-of-plane magnetic hysteresis loops of 4L measured at 2 K and 200 K respectively.

(a)

Compound	Space group	Lattice parameter(Å)	Atomic position
MnSn	*P-62m*	a=6.5764 c=2.9097	Mn(3g): 0.7742, 1.0000, 0.5000 Sn(3f): 0.4156, 1.0000, 0.5000

(b)

	Mn-Mn	Sn-Sn	Mn-Sn
Nearest	2.572	2.910	2.771
Next nearest	2.910	3.426	2.781

Table S1. Details of the DFT optimized MnSn structure. (a) Atomic coordinates of Mn and Sn atoms. (b) The distances of nearest and next nearest neighbor Mn-Mn, Sn-Sn and Mn-Sn atoms (Å).